Biochemical Journal (2021) **478** 3539–3553
https://doi.org/10.1042/BCJ20210629

Research Article

Calpain-2 specifically cleaves Junctophilin-2 at the same site as Calpain-1 but with less efficacy

Jinxi Wang[1], Grace Ciampa[1,2], Dong Zheng[3], Qian Shi[4], Biyi Chen[1], E. Dale Abel[4,5], Tianqing Peng[3], Duane D. Hall[1] and Long-Sheng Song[1,2,5,6]

[1]Division of Cardiovascular Medicine, Department of Internal Medicine, Abboud Cardiovascular Research Center, Carver College of Medicine, University of Iowa, Iowa City, IA 52242, U.S.A.; [2]Department of Biochemistry, Carver College of Medicine, University of Iowa, Iowa City, IA 52242, U.S.A.; [3]Department of Pathology and Laboratory Medicine, University of Western Ontario, London, ON N6A 4S2, Canada; [4]Division of Endocrinology & Metabolism, Carver College of Medicine, University of Iowa, Iowa City, IA 52242, U.S.A.; [5]Fraternal Order of Eagles Diabetes Research Center, Carver College of Medicine, University of Iowa, Iowa City, IA 52242, U.S.A.; [6]Department of Veterans Affairs, Iowa City Medical Center, Iowa City, IA 52242, U.S.A.

Correspondence: Long-Sheng Song (long-sheng-song@uiowa.edu)

Calpain proteolysis contributes to the pathogenesis of heart failure but the calpain isoforms responsible and their substrate specificities have not been rigorously defined. One substrate, Junctophilin-2 (JP2), is essential for maintaining junctional cardiac dyads and excitation-contraction coupling. We previously demonstrated that mouse JP2 is cleaved by calpain-1 (CAPN1) between Arginine 565 (R^{565}) and Threonine 566 (T^{566}). Recently, calpain-2 (CAPN2) was reported to cleave JP2 at a novel site between Glycine 482 (G^{482}) and Threonine 483 (T^{483}). We aimed to directly compare the contributions of each calpain isoform, their Ca^{2+} sensitivity, and their cleavage site selection for JP2. We find CAPN1, CAPN2 and their requisite CAPNS1 regulatory subunit are induced by pressure overload stress that is concurrent with JP2 cleavage. Using *in vitro* calpain cleavage assays, we demonstrate that CAPN1 and CAPN2 cleave JP2 into similar 75 kD N-terminal (JP2NT) and 25 kD C-terminal fragments (JP2CT) with CAPNS1 co-expression enhancing proteolysis. Deletion mutagenesis shows both CAPN1 and CAPN2 require R^{565}/T^{566} but not G^{482}/T^{483}. When heterologously expressed, the JP2CT peptide corresponding to R^{565}/T^{566} cleavage approximates the 25 kD species found during cardiac stress while the C-terminal peptide from potential cleavage at G^{482}/T^{483} produces a 35 kD product. Similar results were obtained for human JP2. Finally, we show that CAPN1 has higher Ca^{2+} sensitivity and cleavage efficacy than CAPN2 on JP2 and other cardiac substrates including cTnT, cTnI and β2-spectrin. We conclude that CAPN2 cleaves JP2 at the same functionally conserved R^{565}/T^{566} site as CAPN1 but with less efficacy and suggest heart failure may be targeted through specific inhibition of CAPN1.

Introduction

Excitation-Contraction (E-C) coupling is the mechanism by which millions of working cardiomyocytes generate rigorous and coordinated Ca^{2+}-dependent myofilament contraction to enable the heart to pump blood throughout the body [1]. During E-C coupling, efficient, uniform and synchronous Ca^{2+} release throughout the cytosol of cardiomyocytes is governed by a process called Ca^{2+}-induced Ca^{2+} release [2–4]. Cardiomyocytes have developed intracellular membrane junctional contacts for mediating Ca^{2+}-induced Ca^{2+} release dubbed cardiac dyads [5]. An exquisite network of specialized plasma membrane structures known as transverse tubules, or T-tubules, make numerous dyadic couplings with the terminal cisternae of sarcoplasmic reticulum (SR) Ca^{2+} stores [5–8]. Thus, upon membrane depolarization within these dyadic Ca^{2+} microdomains, a small amount of Ca^{2+} entry via voltage-gated L-type Ca^{2+} channels triggers a large amount of Ca^{2+} release from the SR via type 2

Received: 23 August 2021
Revised: 14 September 2021
Accepted: 15 September 2021

Accepted Manuscript online: 15 September 2021
Version of Record published: 6 October 2021

Biochemical Journal (2021) 478 3539–3553
https://doi.org/10.1042/BCJ20210629

ryanodine receptors [9–12]. Excessive stress or injury to cardiomyocytes results in defective E-C coupling which reduces pumping capacity and can give rise to the clinical syndrome of heart failure, the leading cause of death worldwide [7,13–18].

Junctophilin 2 (JP2) is required for establishing the 12–15 nm gap junctions between the sarcolemma and SR membranes in the cardiac dyads [19–21], and is essential for maintaining the integrity of T-tubule system [22–26], but is down-regulated in response to cardiac stress [22,27–37]. JP2 down-regulation itself contributes to the development of heart failure as knockdown or deletion of JP2 in cardiomyocytes is sufficient to cause E-C uncoupling and heart failure progression [19,38,39]. Ca^{2+}-dependent activation of calpain proteases are now well accepted to promote E-C uncoupling through the proteolysis of critical dyadic proteins including JP2 [37,40–44]. Several groups reported that JP2 from muscle tissues and heterologously expressing cells appears as a ∼100 kD protein on immunoblots despite having a molecular mass of ∼75 kD [19,28,32,34,44,45]. Ca^{2+}- and calpain-dependent cleavage of JP2 results in the reproducible production of 75- and 25 kD fragments indicating cleavage is site-specific [37,42–44,46,47]. These studies underscore the concerted efforts over the years to better understand how calpain is activated and how it recognizes JP2 in addition to its other substrates.

The identity of the specific calpain(s) responsible for cleaving junctophilins under pathological conditions *in vivo* remains ambiguous. The most understood calpains are μ-Calpain (Calpain-1, CAPN1) and m-Calpain (Calpain-2, CAPN2) that are ubiquitously expressed and activated by autolysis in response to micro-Molar (μM) and milli-Molar (mM) Ca^{2+}, respectively [48,49]. Available calpain inhibitors cannot distinguish between different calpain homologs and definitive animal models have not been reported in the context of junctophilin proteolysis. In cardiac studies thus far, administration of MDL-28170, a calpain inhibitor, or transgenic overexpression of calpastatin, an endogenous inhibitor of calpain proteases, can inhibit JP2 proteolysis during heart failure stress resulting in improved cardiac outcomes [37]. We recently reported that diseased human hearts have elevated calpain activity and cardiac overexpression of CAPN1 in mice is sufficient to promote JP2 degradation and heart failure [37].

We were the first group to evaluate the molecular determinants within JP2 that mediate cleavage by calpains, specifically CAPN1. Cleavage of full-length JP2 in heart lysates from mouse and human is enhanced by addition of CAPN1 and high concentration of Ca^{2+} but inhibited in the presence of the Ca^{2+} chelator EGTA or the peptide calpain inhibitor Z-LLY-FMK [44]. Our previous work found a variety of cardiac stresses initiate site-specific cleavage of JP2 producing a 75 kDa N-terminal fragment (JP2NT) [46]. Through internal deletion mutagenesis, we mapped the primary calpain cleavage site in JP2 to R^{565}/T^{566}. We confirmed that the migration of the corresponding N- and C-terminal peptides aligns with the previously observed 75- and 25 kD proteolytic fragments, respectively [44]. Unexpectedly, we found that N-terminal peptide (JP2NT) contains a nuclear localization sequence (NLS, residues 488–492) that facilitates its robust translocation into cardiomyocyte nuclei in response to transverse aortic constriction (TAC) induced pressure overload and other stresses where it acts to suppress the maladaptive expression of heart failure-related genes [46].

The possibility that CAPN2 is responsible for cleaving JP2 was recently pursued by the Wehrens group reasoning that JP2 remains largely intact in unstressed hearts during normal Ca^{2+} cycling conditions sufficient for CAPN1 activation but only becomes preferentially cleaved during pathological stress when cytosolic Ca^{2+} reaches mM levels [47]. In support of this idea, knockdown of CAPN2 in H9c2 rat atrial cells, but not CAPN1, was as effective as calpastatin in inhibiting the generation of the 25 kD C-terminal proteolytic peptide, referred to as CTP [47]. Interestingly, nuclear puncta were observed in response to extracellular application of Ca^{2+} in JP2 transfected cells that were positive for distal C-terminal epitopes and interpreted as the CTP fragment. This phenomenon requires the JP2 NLS and limited evidence was provided that CTP arises from cleavage at G^{482}/T^{483} just prior to the JP2 NLS ($K^{488}RPRP^{492}$). However, it remains unclear whether CAPN2 specifically recognizes either G^{482}/T^{483} or R^{565}/T^{566} or if either of the corresponding C-terminal fragments form nuclear puncta. Given the requirement of JP2 in E-C coupling, that its proteolysis under cardiac stress contributes to heart failure, and the new debate as to the physiologically relevant calpain isoform and proteolytic site responsible, a more precise understanding of the mechanisms by which JP2 is cleaved by calpains is needed. Therefore, we endeavor here to directly compare CAPN1 versus CAPN2 with respect to their cardiac stress responsiveness, Ca^{2+} sensitivity, JP2 cleavage site specificity, and their effect on JP2 fragment subcellular distribution.

Biochemical Journal (2021) **478** 3539–3553
https://doi.org/10.1042/BCJ20210629

Results

CAPN1 and CAPN2 are up-regulated by TAC and in parallel with increased JP2 cleavage

To begin to resolve the contribution of calpain isoforms in cardiac JP2 proteolysis, we analyzed the time-dependent generation of JP2 proteolytic fragments in response to TAC surgery. Consistent with our published work [46], Western blotting with JP2 antibodies against N- and C-terminal epitopes showed that full-length JP2 is down-regulated while the 75 kD JP2 N-terminal (JP2NT) cleavage product gradually increases during the 1–5 weeks of pressure overload stress in C57BL/6N male mice hearts (Figure 1a–c). Predictably, we also observed an increase in a 25 kD C-terminal product (JP2CT) in this TAC model (Figure 1b,d). A similar migrating band of ∼25 kD was also observed by Lahiri et al. [47] in failing heart lysates using the same JP2 C-terminal antibody. Both CAPN1 and CAPN2 protein levels are significantly elevated compared with the sham group with peak protein abundance occurring during the first 3 weeks of TAC stress and just prior to maximal JP2NT and JP2CT generation (Figure 1b,e,f). These data suggest that either calpain could contribute to JP2 cleavage *in vivo*, particularly during the initial cardiac remodeling stages when E-C coupling dysfunction first appears.

The region spanning mJP2 R^{565}/T^{566}, but not G^{482}/T^{483}, is necessary to form the 75 kD N-terminal and 25 kD C-terminal calpain cleavage products

A striking difference among studies defining calpain-dependent site-specific cleavage of JP2 is that the 25 kD C-terminal calpain cleavage band arises from two different cleavage sites located nearly 80 amino acids apart [44,47]. We proposed that the major site of calpain activity, and for CAPN1 in particular, occurs between residues R^{565} and T^{566}. On the other hand, Lahiri, et al. proposed cleavage by CAPN2 occurs between G^{482} and T^{483}. To directly compare whether CAPN1 and/or CAPN2 can cleave JP2 at G^{482}/T^{483} and/or R^{565}/T^{566}, we created internal JP2 deletions overlapping these sites based on these prior reports [44,47]. For expression and cleavage analysis, we fused mouse JP2 (WT mJP2), $mJP2^{\Delta 479-486}$ and $mJP2^{\Delta 563-568}$ coding sequences with N-terminal FLAG and C-terminal HA tags (Figure 2a). HEK293T cells were co-transfected with dual tagged JP2 constructs with human CAPN1 or CAPN2 expressing plasmids for 24 h. Cell lysates were then used for *in vitro* calpain cleavage assays in the presence and absence of 2 mM Ca^{2+}. Blotting with FLAG and HA antibodies demonstrated that WT mJP2 is proteolyzed by CAPN1 in a Ca^{2+}-dependent manner into the 75 kD JP2NT and 25 kD JP2CT fragments (Figure 2b lanes 1–3). Treatment with the calpain inhibitor MDL-28170 resulted in a substantial reduction in the presence of both the N- and C-terminal cleavage products (Figure 2b lane 4). Deletion of the G^{482}/T^{483} site ($JP2^{\Delta 479-486}$) had no influence on the generation of the 75 kD JP2NT and 25 kD JP2CT peptides by CAPN1, while deletion of the R^{565}/T^{566} site ($JP2^{\Delta 563-568}$) abrogated the formation of both proteolytic bands (Figure 2b lanes 5–12). These data confirm our previously published data [44] that R^{565}/T^{566} is the primary site responsible for CAPN1-dependent generation of the 75 kD JP2NT and 25 kD JP2CT fragments. Furthermore, we find that CAPN2 is also able to cleave JP2 into 75 kD JP2NT and 25 kD JP2CT species in the presence of high Ca^{2+}. As with CAPN1, CAPN2 cleavage of JP2 requires R^{565}/T^{566} but not G^{482}/T^{483} (Figure 2c). These data demonstrate that both CAPN1 and CAPN2 are able to specifically cleave JP2 at the same R^{565}/T^{566} site to form the same cleavage products.

CAPN2 cleavage efficacy for JP2 under optimal Ca^{2+} conditions is lower than that of CAPN1

We noticed that the generation of 75 kD JP2NT and 25 kD JP2CT by CAPN2 may be less efficacious than CAPN1 in the presence of 2 mM Ca^{2+} (compare Figure 2b,c). It has been reported that CAPN1 is activated under μM Ca^{2+} while CAPN2 is activated by mM Ca^{2+}. To better compare the efficacy of CAPN1 and CAPN2 on the cleavage of JP2, we assessed the activity of each exposed to a range of Ca^{2+} concentrations using *in vitro* calpain cleavage assays as above. The formation of 75 kD JP2NT and 25 kD JP2CT by both calpains were dose-dependently increased by Ca^{2+} (Figure 3a,b). However, the cleavage efficacy of CAPN1 for JP2 is more robust and significantly more sensitive to Ca^{2+} than CAPN2 (Figure 3a,b). These data suggest that the efficacy of CAPN2 cleavage on JP2 is much lower than that for CAPN1, even under mM Ca^{2+} conditions.

Calpains operate as heterodimers, comprised of a large ∼75 kD catalytic subunit (CAPN1 or CAPN2), and a common small regulatory subunit CAPNS1, also known as calpain 4. CAPNS1 is essential for the stability and function of both CAPN1 and CAPN2 [50]. To better evaluate and compare the calpain cleavage efficacy on JP2

Biochemical Journal (2021) **478** 3539–3553
https://doi.org/10.1042/BCJ20210629

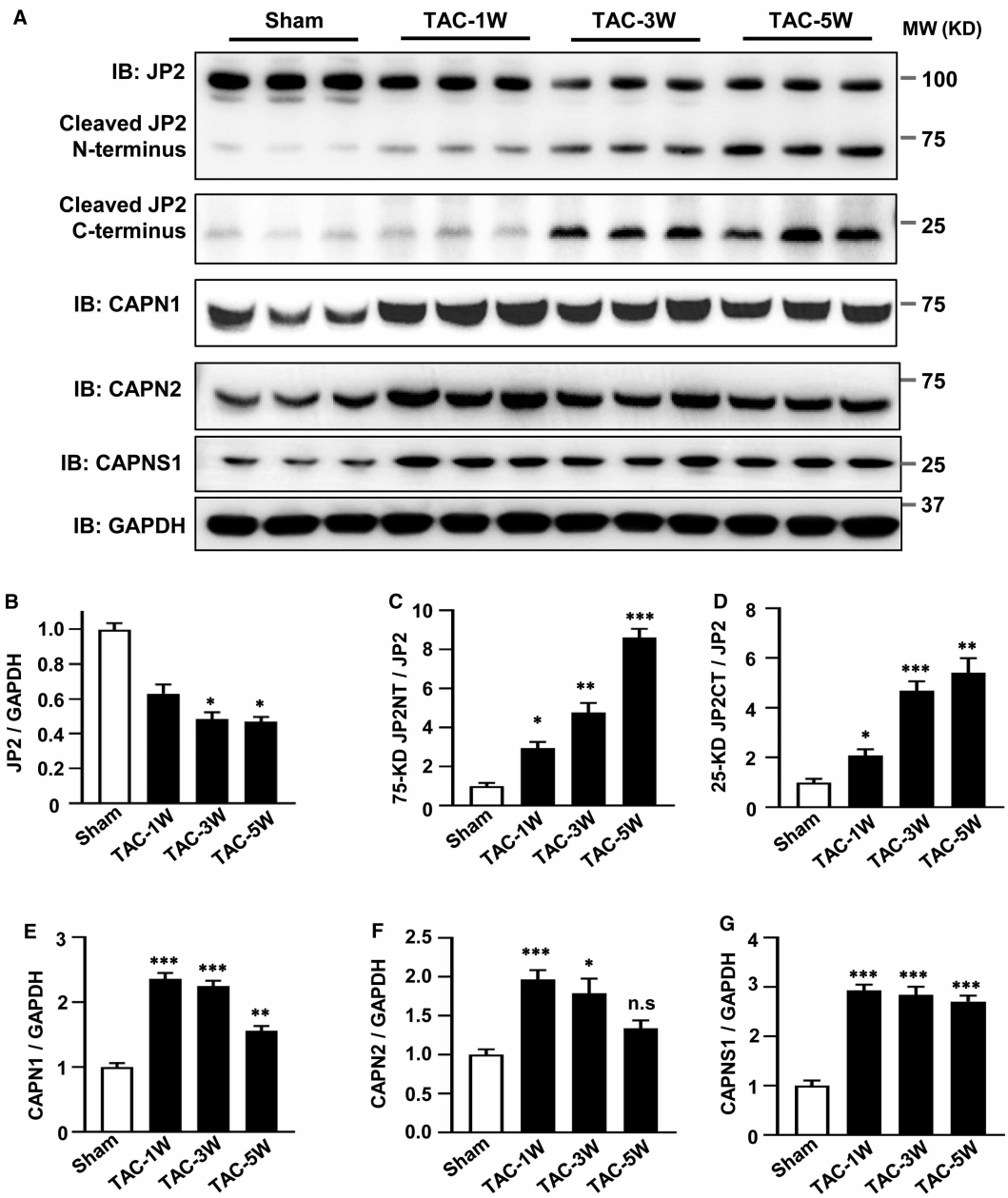

Figure 1. Transverse aortic constriction (TAC) induces cardiac Calpain expression and JP2 cleavage.

(**A**) Representative Western blots of JP2, CAPN1, CAPN2 and CAPNS1 in heart homogenates from sham and TAC operated animals. (**B–D**) Western blot quantification of full-length JP2 relative to GAPDH loading control (**B**) and its ~75 kD N-terminal (**C**) and 25 kD C-terminal (**D**) cleavage products normalized to full-length JP2. (**E–G**) Quantification of CAPN1 (**E**), CAPN2 (**F**) and CAPNS1 (**G**) expression in TAC and Sham hearts normalized to GAPDH. $n = 6$ for each group. Data are mean ± SEM. One-way ANOVA followed by the Tukey multiple-comparisons test. * $P < 0.05$, ** $P < 0.01$, *** $P < 0.001$. n.s., non-significant.

in the context of calpain holoenzymes (CAPN1/CAPNS1 or CAPN2/CAPNS1), we overexpressed CAPNS1 together with JP2 and CAPN1 or CAPN2 in HEK293T cells and performed *in vitro* calpain cleavage assays. As expected, overexpression of CAPNS1 alone had no influence on JP2 cleavage under 50 μM and 500 μM Ca^{2+} conditions while it dramatically promoted the efficiency of CAPN1 and CAPN2 on the cleavage of JP2 (Figure 3c,d). We also observed that even in the presence of CAPNS1, the efficacy of CAPN2 remains lower than

Biochemical Journal (2021) **478** 3539–3553
https://doi.org/10.1042/BCJ20210629

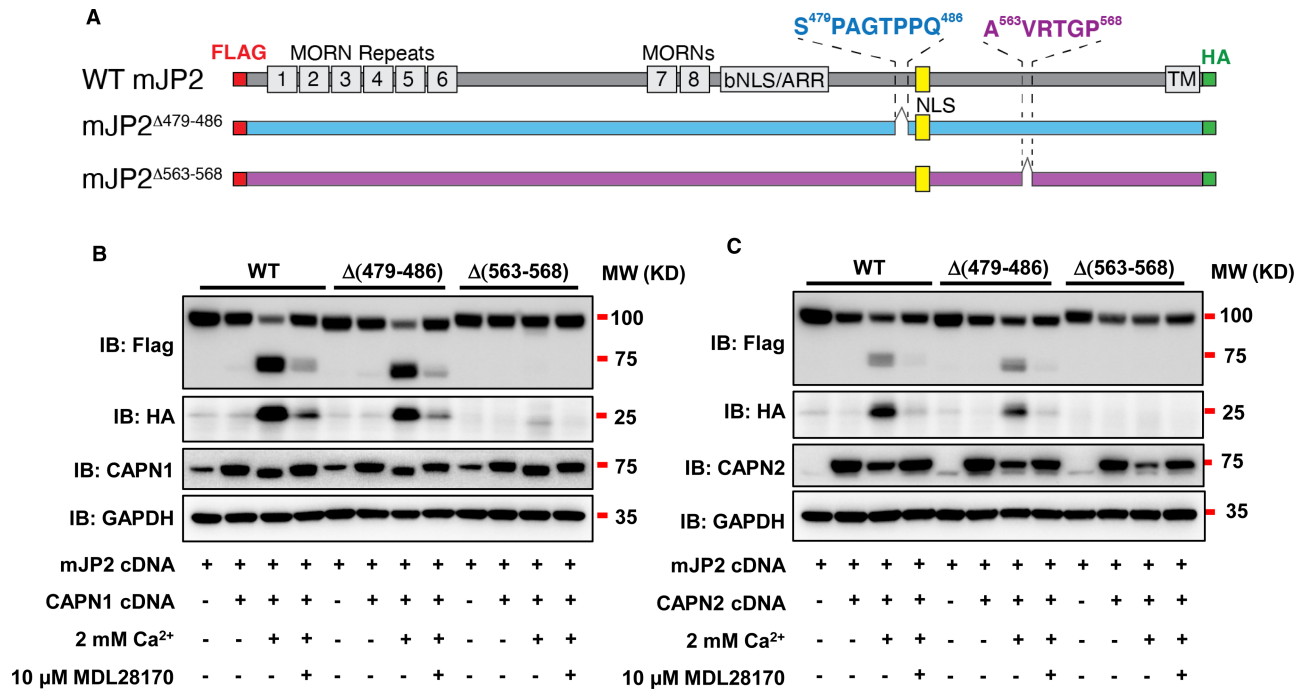

Figure 2. Residues 563–568, but not 479–486 of mouse JP2, are necessary for CAPN1 and CAPN2 to cleave JP2 into 75 kD N-terminal and 25 kD C-terminal fragments.

(**A**) Schematic of Flag- and HA-tagged JP2 deletion constructs used to test calpain cleavage site selection. (**B**,**C**) Western blots of *in vitro* calpain assays. HEK293T cells were co-transfected with mJP2-WT, mJP2$^{\Delta 479-486}$ or mJP2$^{\Delta 563-568}$ and either CAPN1 (**B**) or CAPN2 (**C**) cDNAs for 24 h. Cell lysates were exposed with and without 2 mM Ca^{2+} for 20 min in calpain reaction buffer in the absence or presence of 10 μM MDL-28170 (inhibitor of CAPN1 and CAPN2). JP2 expression and cleavage were assessed with anti-Flag or anti-HA antibodies to detect N- and C-terminal cleavage fragments, respectively.

CAPN1 (Figure 3c,d). Interestingly, smaller proteolytic fragments of CAPNS1 are present when co-expressed with CAPN1 or CAPN2 suggesting it itself is cleaved by calpains under 50 μM and 500 μM Ca^{2+} (Figure 3c,d).

CAPN1 and CAPN2 cleave human JP2 at the site analogous to mouse JP2 R^{565}/T^{566}

We next questioned whether human JP2 (hJP2) undergoes a similar proteolytic process under pathological conditions by CAPN1 and CAPN2. Using online calpain cleavage algorithm (GPS-CCD 1.0 and CaMPDB), we found potential calpain cleavage sites in hJP2 that are homolgous to those in mJP2, i.e. G^{489}/T^{490} and R^{572}/T^{573}. For expression and cleavage analysis, we fused human JP2 (WT hJP2), hJP2$^{\Delta 486-493}$ and hJP2$^{\Delta 570-575}$ coding sequences with N-terminal FLAG and C-terminal HA tags as we did for mJP2 (Figure 4a). We then performed the same *in vitro* calpain cleavage assay in both low (50 μM) and high (2 mM) levels of Ca^{2+}. Western blotting with FLAG and HA antibodies demonstrated that WT hJP2 is proteolyzed by CAPN1 into the 75 kD JP2NT and 20 kD JP2CT fragments (Figure 4b,c, lane 3). Treatment with the calpain inhibitor MDL-28170 resulted in a drastic reduction in both the N- and C-terminal cleavage products (Figure 4b,c, lane 4). Deletion of the G^{489}/T^{490} site (hJP2$^{\Delta 486-493}$) had minimal influence on the generation of the 75 kD JP2NT and 20 kD JP2CT peptides by CAPN1 (Figure 4b) and CAPN2 (Figure 4c), while deletion of the R^{572}/T^{573} site (hJP2$^{\Delta 570-575}$) abrogated the formation of both proteolytic bands completely (Figure 4b,c, lanes 5–12). Similar results were obtained under higher Ca^{2+} concentrations, however both calpains appeared to cleave WT and hJP2$^{\Delta 486-493}$ more readily. Also similar to mJP2, CAPN1 was more efficacious in proteolyzing hJP2 than CAPN2 (Figure 4d,e). These data suggest that hJP2 R^{572}/T^{573} is the primary site responsible for CAPN1- and CAPN2-dependent generation of the 75 kD JP2NT and 20 kD JP2CT fragments in hJP2. Altogether, our data demonstrate that both CAPN1 and CAPN2 are able to specifically cleave JP2 at the same homologous site, i.e. R^{565}/T^{566} (mouse) or R^{572}/T^{573} (human) to form similar cleavage products.

Biochemical Journal (2021) **478** 3539–3553
https://doi.org/10.1042/BCJ20210629

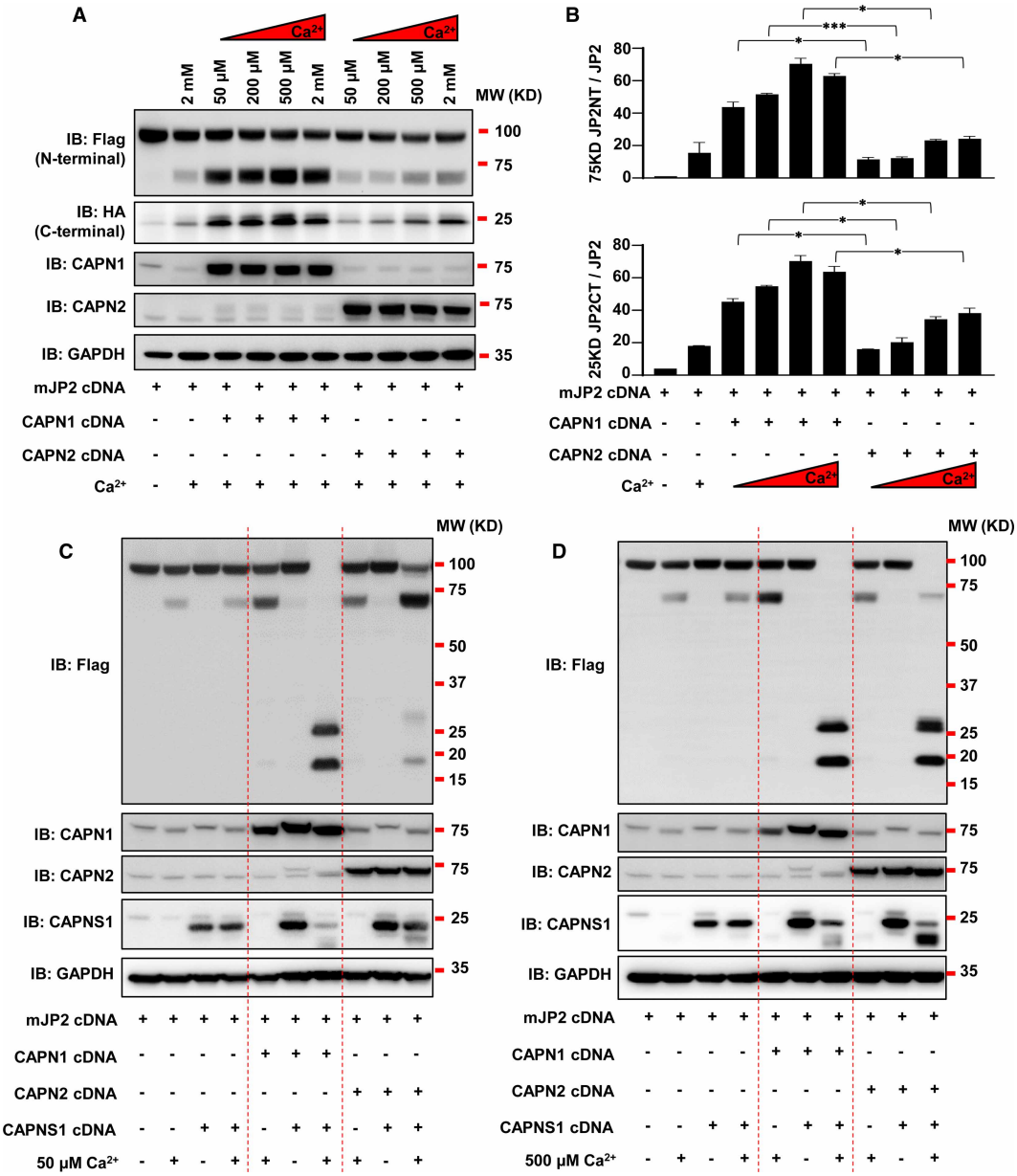

Figure 3. CAPN2 is less efficacious in cleaving JP2 than CAPN1.

(**A**,**B**) Representative Western blots (**A**) and summary data (**B**) of JP2 (mouse species) cleavage assays under different Ca^{2+} ($CaCl_2$) concentrations, as indicated, using cell lysates from HEK293T cells expressing CAPN1 or CAPN2. (**C**,**D**) Western blots of calpain cleavage assays for 10 min in calpain reaction buffer. Lysates from cells overexpressing CAPNS1 in addition to CAPN1 and CAPN2 were exposed to 50 µM (**C**) or 500 µM (**D**) $CaCl_2$, as indicated. JP2 expression and cleavage were assessed by Western blotting with anti-Flag to detect N-terminal cleavage fragments, respectively. $n = 3$ for each group. Data are mean ± SEM. One-way ANOVA followed by the Tukey multiple-comparisons test. * $P < 0.05$, *** $P < 0.001$.

Expression constructs mimicking cleavage at R^{565}/T^{566} but not G^{482}/T^{483} correspond to *in vivo* generated JP2 75 kD N-terminal and 25 kD C-terminal fragments

To distinguish whether the 75 kD JP2NT and 25 kD JP2CT fragments are formed by cleavage at G^{482}/T^{483} versus R^{565}/T^{566}, we generated a panel of C-terminal HA-tagged JP2 truncates on the basis of the different calpain cleavage sites (Figure 5a). When expressed exogenously in HEK293T cells, $JP2^{1-565}$ has a similar

Biochemical Journal (2021) **478** 3539–3553
https://doi.org/10.1042/BCJ20210629

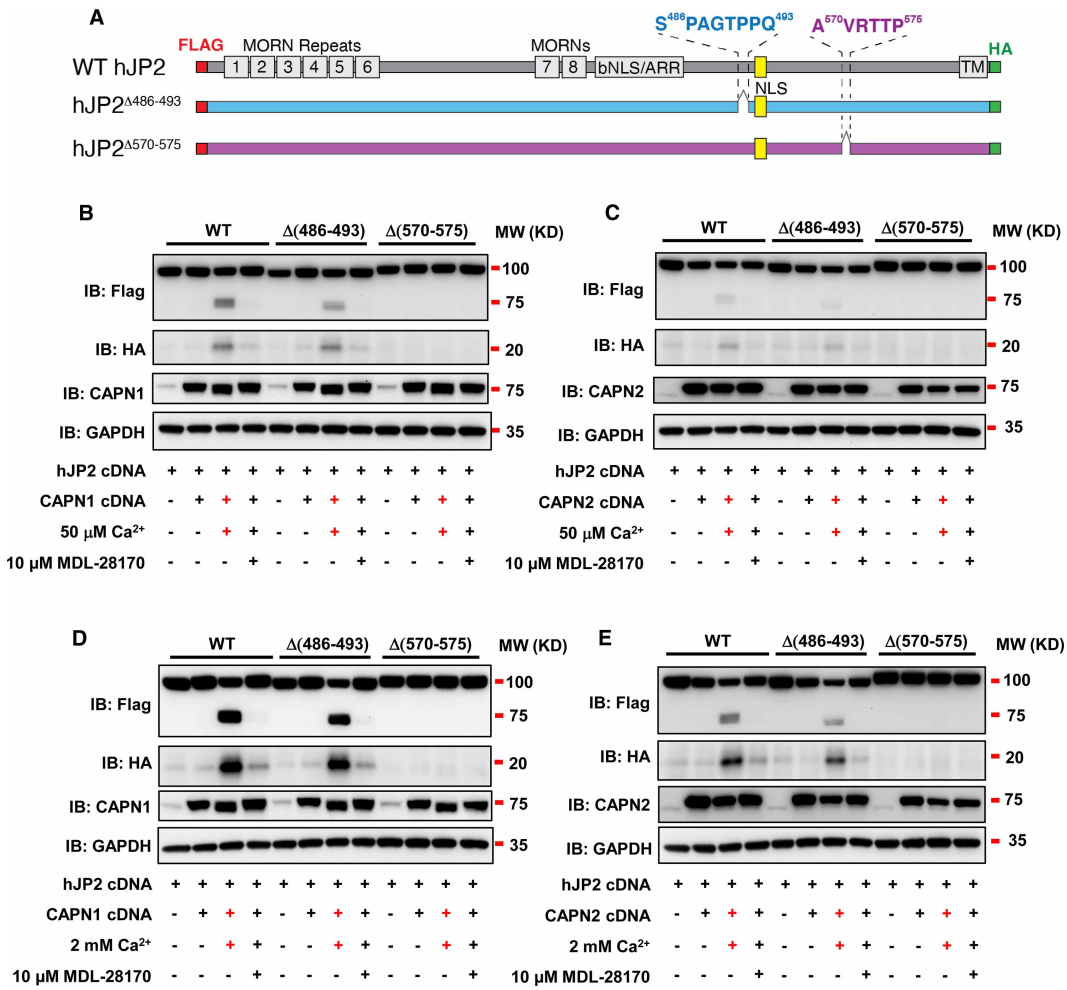

Figure 4. Human JP2 (hJP2) is cleaved by CAPN1 and CAPN2 in the same region analogous to mouse JP2 R^{565}/T^{566}.
(**A**) Schematic of Flag- and HA-tagged human JP2 deletion constructs used to test calpain cleavage site selection. (**B–E**) Western blots of *in vitro* calpain assays. HEK293T cells were co-transfected with hJP2-WT, $hJP2^{\Delta 486-493}$ or $hJP2^{\Delta 570-575}$ and either CAPN1 (**B**,**D**) or CAPN2 (**C**,**E**) cDNAs for 24 h. Cell lysates were exposed with and without 50 μM or 2 mM Ca^{2+} for 20 min in calpain reaction buffer in the absence or presence of 10 μM MDL-28170. Human JP2 expression and cleavage were assessed with anti-Flag or anti-HA antibodies to detect N- and C-terminal cleavage fragments, respectively.

molecular mass as the 75 kD band we found induced by TAC *in vivo* (Figure 1a), expressed previously from a different vector, [44] and expressed *in vivo* as JP2NT. [46] Expression of $JP2^{1-482}$ produces a smaller protein with a molecular mass of ~65 kD. Note that $JP2^{566-696}$, which is the C-terminal counterpart of $JP2^{1-565}$, has a similar molecular mass as the 25 kD JP2CT after TAC (Figure 1a) while the proposed CTP peptide ($JP2^{483-696}$) runs with an larger apparent molecular mass of ~35 kD.

To validate these findings, we immunoblotted lysates using our custom made JP2 antibody that effectively detects all N-terminal JP2 species (full-length JP2, $JP2^{1-482}$, and $JP2^{1-565}$). The commercial C-terminal JP2 antibody not only detects the C-terminal JP2 truncates ($JP2^{483-696}$, $JP2^{566-696}$) and full-length JP2 but also recognizes $JP2^{1-565}$ (Figure 5b). Additionally, the N-terminal JP2 antibody can specifically detect 75 kD JP2NT, while the C-terminal JP2 antibody not only detects a 25 kD peptide but also a 75 kD fragment in TAC heart lysates compared with sham controls (Figure 5c). These results indicate the C-terminal JP2 antibody used by the Wehrens group is not a perfect tool in distinguishing possible N- versus C-terminal JP2 products [47]. Cumulatively, these direct comparisons indicate the 75 kD JP2NT and 25 kD JP2CT fragments are more likely generated by a single cleavage of JP2 at R^{565}/T^{566} rather than Gly^{482}/T^{483}.

Biochemical Journal (2021) **478** 3539–3553
https://doi.org/10.1042/BCJ20210629

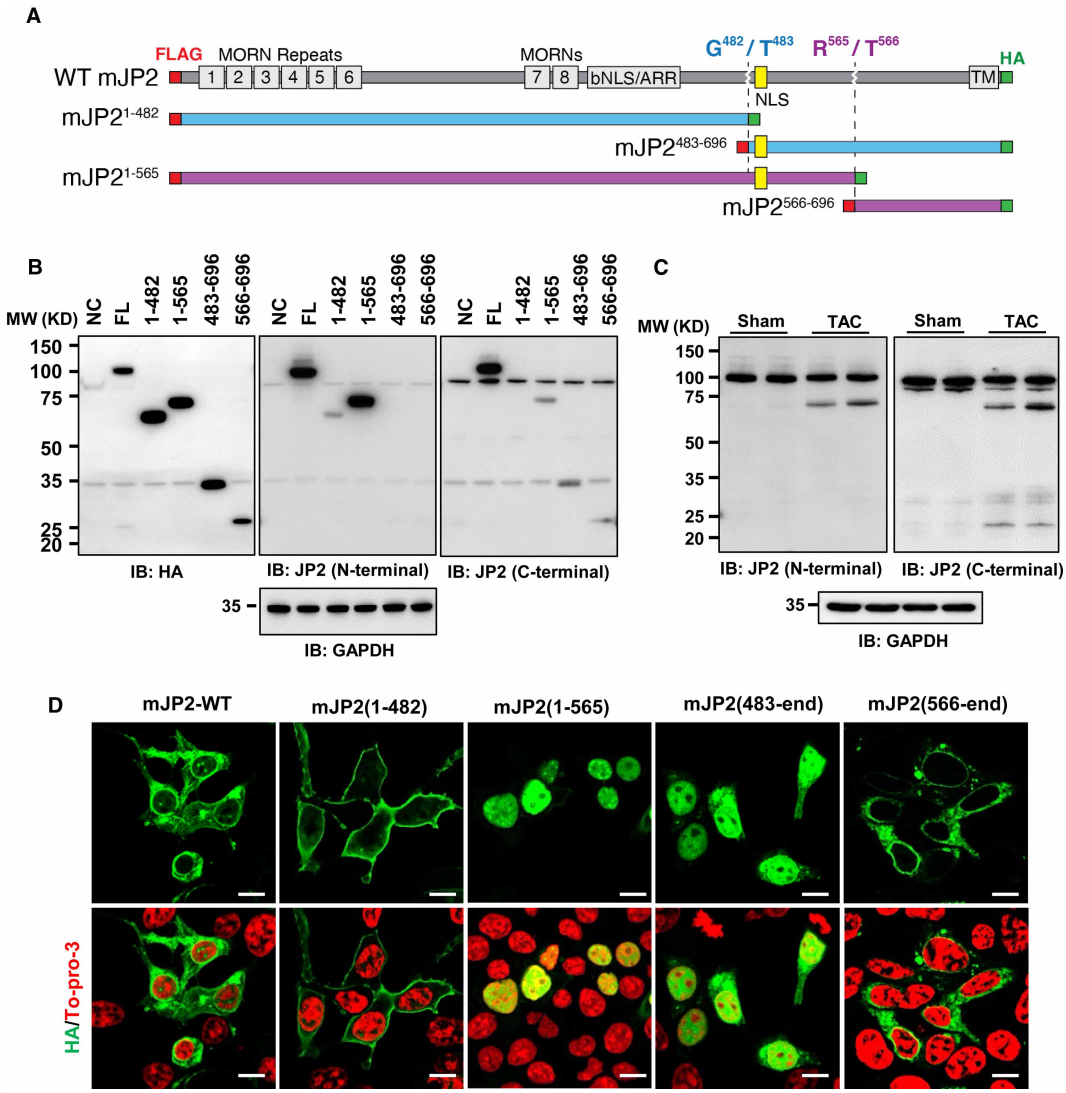

Figure 5. Expression constructs mimicking cleavage at mouse JP2 R^{565}/T^{566}, but not G^{482}/T^{483}, reconstitute the proteolytic and nuclear localization patterns of JP2.

(**A**) Schematic of N- and C-terminal epitope-tagged JP2 expression constructs for comparing putative calpain cleavage sites. (**B**) Expression of JP2 constructs in HEK293T cells detected by HA, JP2 N-terminal and JP2 C-terminal antibodies. NC, negative control; FL, full length. (**C**) Western blots for JP2 cleavage in Sham versus TAC operated hearts after 1 week using antibodies recognizing N- and C-terminal JP2 sequences. (**D**) Immunofluorescent localization of C-terminal HA-tagged JP2 expression constructs relative to TO-PRO-3 stained DNA in HEK293T cells. Scale bar = 10 μm.

As JP2, JP2NT and CTP possess the JP2 NLS, we next expressed the different JP2 truncates in HEK293 cells to examine their subcellular distribution by immunofluorescence (IF). In line with our previous work [46], JP2NT ($JP2^{1-565}$) exclusively localizes in the nucleus (Figure 5d). While most of CTP ($JP2^{483-696}$) also localizes in the nucleus (Figure 5d), its diffused pattern in nuclei is unlike the punctate pattern reported [47]. Interestingly, we did observe a punctate HA signal inside the nucleus of some full-length JP2 transfected cells growing under normal media conditions. We will expand more on these findings in the Discussion section.

CAPN1 has higher cleavage efficacy than CAPN2 for canonical substrates including cardiac troponin T (TnT), troponin I (cTnI) and β2-spectrin

In addition to JP2, many other cardiac proteins, such as spectrin, cTnT and cTnI, are cleaved by calpain under different cardiac stresses, including ischemia and pressure overload [41,51,52]. To examine the relative activity

Biochemical Journal (2021) 478 3539–3553
https://doi.org/10.1042/BCJ20210629

of the calpain isoforms for these classic substrates, we co-transfected HEK293T cells with CAPN1 or CAPN2 and full-length, dual-tagged β2-spectrin, cTnT and cTnI. 24 h after co-transfection, cell lysates were used for *in vitro* calpain cleavage assays at different Ca^{2+} levels from μM to mM. The formation of cleaved β2-spectrin, cTnT and cTnI by CAPN1 and CAPN2 increased as Ca^{2+} level increase from μM to mM concentration (Figure 6). Similar to JP2, the cleavage efficacy of CAPN1 for these proteins is much higher than CAPN2 across all Ca^{2+} concentrations and is particularly striking for β2-spectrin and cTnT (Figure 6). Taken together, these data demonstrate that the efficacy of CAPN2 cleavage on calpain substrates is lower than CAPN1 under Ca^{2+} levels that allow for maximal activation.

Discussion

In this study, we systemically compared the requirements for the Ca^{2+}-dependent cleavage of JP2 by calpain to resolve the debate surrounding the efficacy and sequence specificity of calpain isoforms for JP2. First, we confirmed that cardiac stress leads to the generation of 75 kD N-terminal and 25 kD C-terminal proteolytic fragments that is preceded by the induction of both CAPN1 and CAPN2. Second, we confirmed that mJP2 is cleaved at R^{565}/T^{566}, and not at G^{482}/T^{483} as recently proposed, and peptides arising from cleavage at this site do, in fact, correspond to 75 kD JP2NT and 25 kD JP2CT fragments. Third, we found that both CAPN1 and CAPN2 isoforms can cleave mJP2 at the same R^{565}/T^{566} site, but not at the G^{482}/T^{483} site. Fourth, we found that the 25 kD JP2CT fragment generated by cleavage at R^{565}/T^{566} cannot translocate into the nucleus because it lacks a nuclear localization sequence. Fifth, we also demonstrate that human JP2 is similarly cleaved by CAPN1 and CAPN2 at the site analogous to mouse JP2 R^{565}/T^{566}. Finally, we found CAPN1, independent of Ca^{2+} concentration, has significantly higher cleavage efficacy for JP2 and other calpain substrates than does CAPN2.

Dramatic and prolonged increases of cytosolic Ca^{2+} in ischemic and hypertrophic conditions have long been known to disrupt E-C coupling in cardiomyocytes [53]. Ca^{2+}-dependent activation of calpain proteases are now widely accepted to promote E-C uncoupling through the proteolysis of critical dyadic proteins including JP2. The most understood calpains are μ-Calpain (CAPN1) and m-Calpain (CAPN2) that are ubiquitously expressed and activated by autolysis in response to μM and mM [Ca^{2+}], respectively [48,49]. Over the last several years, our group has endeavored to better understand the mechanisms involved in calpain-mediated proteolysis of JP2 using CAPN1 as an exploratory tool within *in vitro* cleavage assays. As described above, we originally identified the major JP2 cleavage event occurs at R^{565}/T^{566} [44]. We focused on this site after it was suggested by two different *in silico* algorithms (GPS-CCD 1.0 and CaMPDB). At that time, we presented evidence that mutation of R^{565}/T^{566} blocked the major cleavage event and heterologous expression of the corresponding cleavage products as independent proteins mimicked the size of the proteolyzed bands on Western blots. Furthermore, we observed minor cleavage products that appeared to be further generated from the JP2 N-terminus. After testing candidate calpain sites, we validated minor cleavage occurs at V^{155}/R^{156} and L^{201}/L^{202} [44], the latter of which we identified from failing hearts using mass spectrometry [43].

The report by Lahiri, et al. claimed that the 25 kD JP2CT fragment of JP2 is due to cleavage by CAPN2 just prior to the NLS at G^{482}/T^{483}, not R^{565}/T^{566} [47]. Our prior publications that support R^{565}/T^{566} as the primary cleavage site of JP2 [44,46], however, a direct comparison between G^{482}/T^{483} and R^{565}/T^{566} was not performed by Lahiri et al. [47]. In their study, R^{565}/T^{566} was ruled out as a potential site as it was not expected to be detected by the C-terminal antibody and it was reasoned that no peptide with a predicted mass below 20 kD would run at 25 kD by SDS–PAGE. We show here that the same C-terminal antibody used by the Wehrens group (Thermo Fisher Scientific, #40-5300) is able to detect both the 25 kD and 75 kD fragments (Figure 5b) suggesting multiple epitopes likely span the cleavage site of R^{565}/T^{566}. In supplemental materials, Lahiri et al. [47] indicated this antibody was raised against residues 568–580. We attempted to validate the exact epitope but could not find this information in the product literature and technical support of Thermo Fisher Scientific only affirmed that a peptide in the general vicinity of this sequence was used as an immunogen. JP2 has a molar mass of 75 kD yet is well known to run anomalously at ∼100 kD that may in part be due to palmitoylation [45] and other unknown mechanisms. We have clearly showed here (Figure 5b) and in our previous studies [44] that $JP2^{566–696}$ migrates closer to 25 kD despite having a calculated mass here of 16 kD that includes ∼2 kD from its FLAG and HA tags. We now show that $JP2^{483–696}$ appears as a 35 kD protein, considerably larger than its expected size of 25 kD.

In Figure 2 of Lahiri, et al. [47] deletion of two or eight residues flanking G^{482}/T^{483} appear to reduce, but not eliminate, the production of the 25 kD JP2 product in lysates exposed to Ca^{2+} (2 mM). However, this experiment is difficult to interpret as it lacked important controls (e.g. calpain inhibition or cleavage of

Biochemical Journal (2021) **478** 3539–3553
https://doi.org/10.1042/BCJ20210629

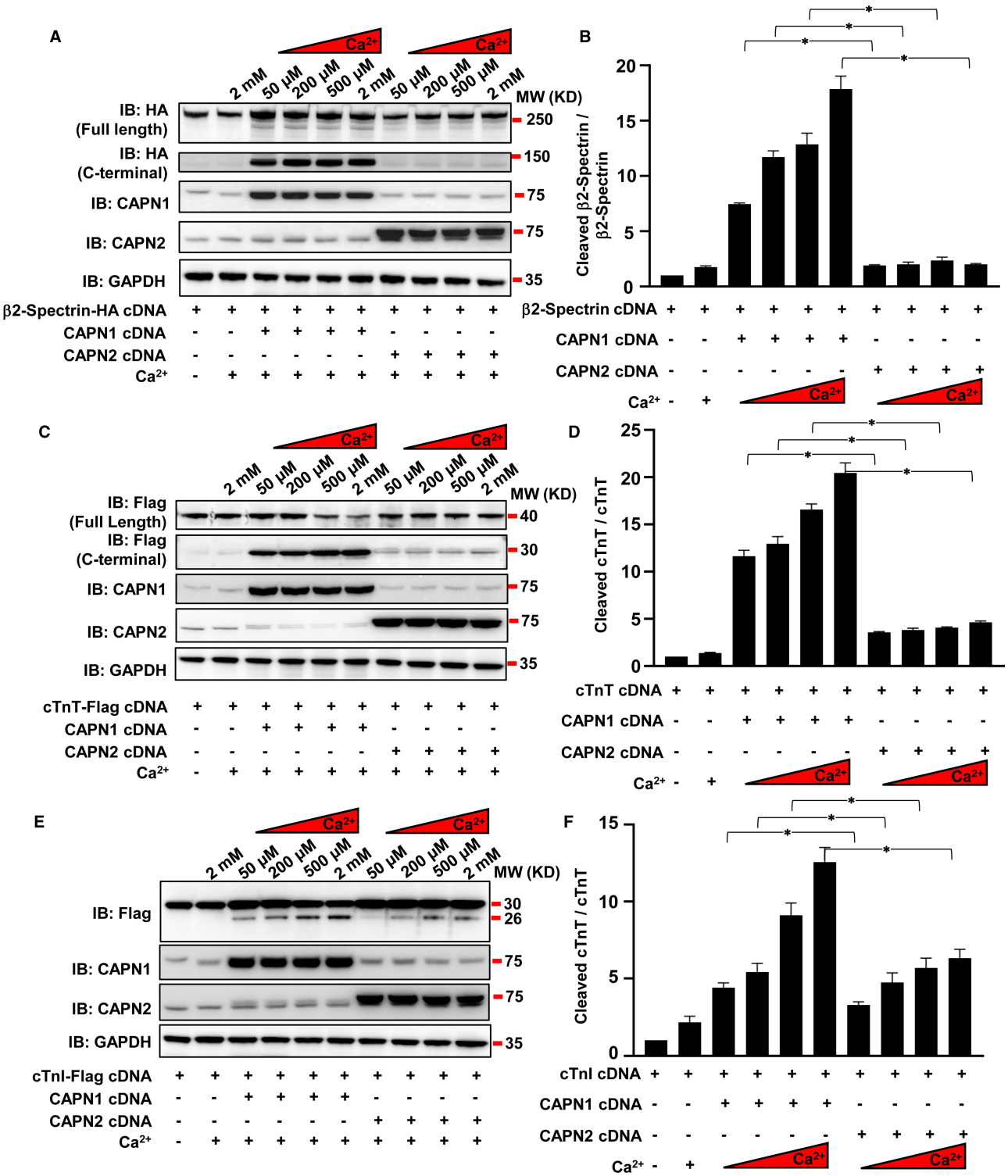

Figure 6. CAPN1 has greater cleavage efficacy than CAPN2 for canonical cardiac substrates.

Representative Western blots and quantification of *in vitro* β2-Spectrin (**A**,**B**), cardiac troponin T (cTnT) (**C**,**D**), and cardiac troponin I (cTnI) (**E**,**F**) cleavage assays in response to CAPN1 and CAPN2 expression and different Ca^{2+} concentrations. Assays were performed as indicated and as described in Figure 4. $n = 3$ for each group. Data are mean ± SEM. One-way ANOVA followed by the Tukey multiple-comparisons test. * $P < 0.05$.

mutated JP2 in the presence or absence of Ca^{2+}). Furthermore, the relative expression of the mutant JP2 constructs is lower than that for wild-type JP2. To better understand the relevance of the G^{482}/T^{483} and R^{565}/T^{566} sites we performed analogous experiments directly comparing the contributions of the two sites on JP2 to be cleaved. In our hands, elimination of G^{482}/T^{483} had no effect on Ca^{2+}-dependent cleavage of JP2 by either CAPN1 or CAPN2 while R^{565}/T^{566} was absolutely required (Figure 2). As expected, excluding Ca^{2+} or inhibiting calpain activity with MDL-28170 similarly attenuated the cleavage of wild-type mJP2 and $mJP2^{\Delta 479-486}$ by both calpains.

Our data demonstrating that G^{482}/T^{483} is not recognized by either CAPN1 or CAPN2 has implications for the identity of JP2 species found in nuclei. After directly comparing the subcellular localization of the various predicted cleavage products (Figure 5d), we confirm our previous report that JP2NT ($JP2^{1-565}$) readily traffics to the nucleus. As predicted by the Wehrens group, we observe that a large fraction of the $JP2^{483-696}$ CTP fragment is nuclear. However, $JP2^{483-696}$ appears diffuse similar to that of JP2NT rather than punctate as originally suggested. Lahiri et al. [47] did not directly visualize CTP by heterologous expression, but rather studied C-terminal HA-tagged full-length JP2 (with and without its NLS) in response to extracellular Ca^{2+} alone. It is possible the punctate nuclear anti HA signal observed in that study could be arising from a different JP2 species. We also observe C-terminal HA-positive puncta in a subset of cells expressing full-length JP2 (Figure 5d). In a recent report by Guo and colleagues, [54] similar appearing nuclear puncta form in cells transfected with full-length JP2 that are positive for both its N-terminal GFP and C-terminal HA tags. Taken together, these findings support the notion that the C-terminal positive nuclear puncta reported by Lahiri et al. [47] are not likely a C-terminal product due to specific cleavage at G^{482}/T^{483} but arise, rather, from a small pool of fully intact JP2. The physiological relevance of nuclear enriched JP2 versus JP2NT after specific cleavage at R^{565}/T^{566} remains to be fully discerned. However, our prior work shows that overexpression of full-length JP2 in cultured cardiomyocytes has minimal impact on cardiomyocyte gene transcription, while JP2NT expression suppresses a wide spectrum of heart failure-related genes involved in pro- hypertrophic, -fibrotic, and -inflammatory signaling pathways. Furthermore, cardiac JP2NT overexpressing mice are protected from TAC-induced dysfunction and maladaptive transcriptional remodeling while NLS-deficient JP2 knockin mice have an exaggerated heart failure response [46].

Finally, we addressed whether there are differences in CAPN1 and CAPN2 cleavage efficacy for mouse versus human JP2 and for other calpain targeted cardiac proteins. Pressure overload stress significantly induced CAPN1, CAPN2 and CAPNS1 within 1 week corresponding to JP2 proteolysis. A significant increase in CAPN2 and modest but insignificant elevation in CAPN1 expression was also observed by the Wehrens group after 8 weeks of prolonged TAC stress. The possibility that either calpain could mediate JP2 proteolysis spurred us to examine CAPN1 versus CAPN2 substrate specificity in a cell culture model. Consistent with its micromolar requirement for Ca^{2+}, we observed efficient cleavage of JP2, β2-spectrin, cTnT and cTnI at the lowest Ca^{2+} concentration tested (50 μM) in lysates from CAPN1 overexpressing cells (Figs. 3, 6). Although CAPN2 requires mM Ca^{2+}, the degree to which any of these proteins is cleaved in lysates from CAPN2 overexpressing cells in the presence of 2 mM Ca^{2+} was not as great as CAPN1 at any Ca^{2+} concentration. We also co-expressed the CAPNS1 regulatory subunit to maximally activate heterologously the catalytic subunits and to overcome the possibility that endogenous CAPNS1 levels were rate-limiting. JP2 proteolysis was more robust under these circumstances, however CAPN2 still did not appear to be as effective as CAPN1 (Figure 3c,d). Specific cleavage of mouse JP2 at its $AVR^{565}/T^{566}GP$ motif and the greater efficacy of CAPN1 over CAPN2 in this event appears to be conserved between mice and humans. Mutation of the analogous site in human JP2 also prevented cleavage (Figure 4). In neither species did we observe CAPN1 or CAPN2 mediated proteolysis through the $SPAG^{482}/T^{483}PPQ$ motif.

In summary, we have provided strong evidence that JP2 is cleaved by CAPN1 and CAPN2 at the same site, specifically at R^{565}/T^{566}, in a manner consistent with the pattern observed in heart failure. We have systematically evaluated whether the proposed G^{482}/T^{483} and/or R^{565}/T^{566} sites are responsible for this cleavage. In side-by-side experiments, mutation of R^{565}/T^{566} abolishes while disruption of G^{482}/T^{483} permits JP2 cleavage by either CAPN1 or CAPN2. Even though a C-terminal construct from hypothetical cleavage at G^{482}/T^{483} is able to localize to the nucleus, its sub-nuclear distribution is distinct from previously proposed. Through such comparative analyses, we find no experimental evidence that CAPN1 or CAPN2 is dependent on G^{482}/T^{483} for proteolyzing JP2. In conclusion, through these parallel, comparative and systematic experiments, we demonstrate that CAPN2 cleaves JP2 at the same site as CAPN1 albeit with less efficacy. Altogether, our findings suggest specific targeting of CAPN1 may be of therapeutic benefit for heart failure treatment.

PORTLAND PRESS

Biochemical Journal (2021) **478** 3539–3553
https://doi.org/10.1042/BCJ20210629

Experimental procedures

Animals

Animal experiments were performed in accordance with the Guide for the Care and Use of Laboratory Animals (National Institutes of Health publication 85–23, revised 1996) and were approved by the Institutional Animal Care and Use Committee at the University of Iowa. Transverse aortic constriction (TAC) models were established using male C57BL/6N mice (9 to 10 weeks of age).

Molecular cloning and mutagenesis

All cDNAs were cloned into pCMV6-XL5 and expressed under the control of its CMV promoter. Wild-type mouse JP2 cDNA was provided by Dr. Hiroshi Takeshima (Kyoto University, Japan). Oligonucleotides with FLAG and HA epitope tag sequences were added in frame to the 5′ and 3′ ends, respectively, of the JP2 constructs by PCR. The dual epitope-tagged PCR products of JP2 included full-length JP2 and truncated $JP2^{1-565}$ (JP2NT), $JP2^{566\text{-end}}$ (JP2CT), $JP2^{1-482}$, and $JP2^{483\text{-end}}$ (CTP). The cDNA of human JP2 (Origene, RC219661) was also fused with N-terminal Flag and C-terminal HA tags. Deletion of the reported calpain sites within full-length mouse JP2 and their analogous residues in human JP2 were performed through site directed mutagenesis using QuikChange II (Agilent). The cDNA of CAPNS1 was cloned by PCR from HEK293T cDNA. The pCMV6-XL5-CAPN1 and pCMV6-entry-CAPN2 plasmids expressing human CAPN1 and CAPN2 were provided by Dr. Tianqing Peng (Western University, Canada). cDNA of human cTnT (Origene, RC201218), human cTnI (Origene, RC214740) were fused with C-terminal Flag tag and human β2-Spectrin (Addgene, #31070) were fused with C-terminal HA tag.

In vivo TAC model construction

Nine to 10-week-old male C57BL/6N mice were subjected to pressure overload by TAC surgery, as described previously [23]. Briefly, mice were anesthetized with ketamine/xylazine (100 mg/kg / 5 mg/kg) by i.p. Aortic constriction was performed by tying a 7–0 nylon suture ligature against a 27-gauge needle. For the sham group, the aortic arch was visualized but not banded. Transthoracic echocardiograms were performed on conscious mice in the University of Iowa Cardiology Animal Phenotyping Core Laboratory, using a Vevo 2100 Imager (Visual Sonics), as described previously [23]. Mice were killed 7, 21 or 35 days after TAC or sham surgery with ketamine/xylazine (100 mg/kg / 5 mg/kg) by i.p.

In vitro Calpain-mediated proteolysis reaction

HEK293T cells were obtained from the ATCC and cultured according to the protocol of the manufacturer. All cDNAs were transfected into HEK293T cells by using jetPRIME Transfection reagent according to the protocol of the manufacturer. Briefly, for six-well plates, 2 μg of cDNA was mixed with 200 μL jetPRIME buffer for 10 s and jetPRIME reagent was added to the mix based on the DNA/jetPRIME reagent ratio of 1 : 2 and vortexed for 1 s. Ten minutes later, the transfection mix was added to the medium of HEK293T cells at 60–80% confluency. Cells overexpressing tagged JP2, cTnT, cTnI, β2-spectrin, CAPN1, CAPN2 and CAPNS1 were washed with PBS and homogenized in lysis buffer (20 mM Tris–HCl, 150 mM NaCl, 2 mM EDTA, and 1% Triton X-100), followed by sonication. Homogenates were centrifuged for 15 min at 13 000 rpm at 4°C. Cell extracts were added into ice-cold calpain reaction buffer (to a final concentration of 135 mM NaCl, 5 mM KCl, 1 mM $MgCl_2$, 10 mM glucose, 10 mM Hepes (pH 7.25), 0.3 μM MG132, and 10 mM 2-mercaptoethanol). Just prior to starting the calpain reaction, $CaCl_2$ was added to achieve a final concentration of 50 μM, 200 μM, 500 μM or 2 mM free Ca^{2+} (in the presence of EDTA), as calculated by Winmax32 version 2.50 (Chris Patton, Stanford University, U.S.A.; http://www.stanford.edu/~cpatton/maxc.html). Reactions without Ca^{2+} or without CAPN1 or 2 were used as controls. As an inhibitor of calpain, the final concentration of 10 μM MDL-28170 was added into reactions as indicated. Reactions were incubated at 30°C for the indicated time (10 or 20 min) and stopped by adding EDTA to a final concentration of 10 mM. The reaction products were mixed with 4× LDS Sample Buffer (Thermo Fisher Scientific, NP0007) and 10× Sample Reducing Agent (Thermo Fisher Scientific, NP0004), incubated at 95°C for 5 min and then subjected to Western blotting.

Western blotting

Western blotting was performed as described previously [44]. The antibody used for detecting JP2NT was custom made by Pacific Immunology Inc (N-terminal epitope). Commercially available antibodies were used to

detect the JP2 C-terminus (C-terminal epitope, Thermo Fisher Scientific, #40-5300), Flag (Sigma–Aldrich, #F1804), HA tag (Cell Signaling, #3724), CAPN1 (Cell Signaling, #2556S), CAPN2 (Cell Signaling, #2539S), CAPNS1 (Abcam, # ab92333), and GAPDH (Cell Signaling, #5174).

Statistics

Data are expressed as mean ± SEM. One-way ANOVA followed by the Tukey multiple-comparisons test were applied for paired comparisons. Values of $P < 0.05$ were considered statistically significant.

Data Availability

All data are contained within the manuscript.

Competing Interests

The authors declare that there are no competing interests associated with the manuscript.

Funding

This work was supported by the Albaghdadi Family Medical Foundation and Department of Veterans Affairs of the United States I01-BX002334 (L.S.S.).

CRediT Author Contribution

Long-Sheng Song: Conceptualization, Formal analysis, Supervision, Funding acquisition, Validation, Investigation, Project administration, Writing — review and editing. **Jinxi Wang:** Conceptualization, Formal analysis, Supervision, Funding acquisition, Validation, Investigation, Methodology, Writing – original draft, Project administration, Writing — review and editing. **Grace Ciampa**: Conceptualization, Formal analysis, Investigation, Methodology, Writing — original draft. **Dong Zheng:** Resources, Investigation, Methodology, Writing — original draft. **Qian Shi:** Resources, Formal analysis, Investigation. **Biyi Chen:** Formal analysis, Investigation. **E. Dale Abel:** Formal analysis, Investigation, Writing — review and editing. **Tianqing Peng:** Resources, Writing — review and editing. **Duane Hall:** Resources, Formal analysis, Investigation, Writing — review and editing.

Abbreviations

Ca^{2+}, Calcium; CAPN1, Calpain-1 (μ-Calpain); CAPN2, Calpain-2 (m-Calpain); CAPNS1, Calpain small regulatory subunit (also named as CAPN4); cTnI, Cardiac troponin I; cTnT, Cardiac troponin T; CTP, C-terminal peptide; E-C, Excitation-Contraction (coupling); JP2, Junctophillin-2; JP2CT, C-terminal fragment of JP2; JP2NT, N-terminal fragment of JP2; NLS, Nuclear localization signal or sequence; SR, Sarcoplasmic reticulum; TAC, Transverse aortic constriction.

References

1 Bers, D.M. (2002) Cardiac excitation-contraction coupling. *Nature* **415**, 198–205 https://doi.org/10.1038/415198a
2 Fabiato, A. (1985) Time and calcium dependence of activation and inactivation of calcium-induced release of calcium from the sarcoplasmic reticulum of a skinned canine cardiac purkinje cell. *J. Gen. Physiol* **85**, 247–289 https://doi.org/10.1085/jgp.85.2.247
3 Cannell, M.B., Cheng, H. and Lederer, W.J. (1995) The control of calcium release in heart muscle. *Science* **268**, 1045–1049 https://doi.org/10.1126/science.7754384
4 Eisner, D.A., Caldwell, J.L., Kistamas, K. and Trafford, A.W. (2017) Calcium and excitation-contraction coupling in the heart. *Circ. Res.* **121**, 181–195 https://doi.org/10.1161/CIRCRESAHA.117.310230
5 Fawcett, D.W. and McNutt, N.S. (1969) The ultrastructure of the cat myocardium. I. Ventricular papillary muscle. . *J. Cell Biol.* **42**, 1–45 https://doi.org/10.1083/jcb.42.1.1
6 Brette, F. and Orchard, C. (2003) T-tubule function in mammalian cardiac myocytes. *Circ. Res.* **92**, 1182–1192 https://doi.org/10.1161/01.RES.0000074908.17214.FD
7 Guo, A., Zhang, C., Wei, S., Chen, B. and Song, L.S. (2013) Emerging mechanisms of T-tubule remodelling in heart failure. *Cardiovasc. Res.* **98**, 204–215 https://doi.org/10.1093/cvr/cvt020
8 Hong, T. and Shaw, R.M. (2017) Cardiac T-tubule microanatomy and function. *Physiol. Rev.* **97**, 227–252 https://doi.org/10.1152/physrev.00037.2015
9 Lopez-Lopez, J.R., Shacklock, P.S., Balke, C.W. and Wier, W.G. (1995) Local calcium transients triggered by single L-type calcium channel currents in cardiac cells. *Science* **268**, 1042–1045 https://doi.org/10.1126/science.7754383
10 Stern, M.D., Song, L.S., Cheng, H., Sham, J.S., Yang, H.T., Boheler, K.R. et al. (1999) Local control models of cardiac excitation-contraction coupling. A possible role for allosteric interactions between ryanodine receptors. *J. Gen. Physiol* **113**, 469–489 https://doi.org/10.1085/jgp.113.3.469
11 Wang, S.Q., Song, L.S., Lakatta, E.G. and Cheng, H. (2001) Ca^{2+} signalling between single L-type Ca^{2+} channels and ryanodine receptors in heart cells. *Nature* **410**, 592–596 https://doi.org/10.1038/35069083

Biochemical Journal (2021) **478** 3539–3553
https://doi.org/10.1042/BCJ20210629

12 Song, L.S., Sham, J.S., Stern, M.D., Lakatta, E.G. and Cheng, H. (1998) Direct measurement of SR release flux by tracking 'Ca^{2+} spikes' in rat cardiac myocytes [In process citation]. *J. Physiol. (Lond)* **512**, 677–691 https://doi.org/10.1111/j.1469-7793.1998.677bd.x
13 Gomez, A.M., Valdivia, H.H., Cheng, H., Lederer, M.R., Santana, L.F., Cannell, M.B. et al. (1997) Defective excitation-contraction coupling in experimental cardiac hypertrophy and heart failure. *Science* **276**, 800–806 https://doi.org/10.1126/science.276.5313.800
14 Gomez, A.M., Guatimosim, S., Dilly, K.W., Vassort, G. and Lederer, W.J. (2001) Heart failure after myocardial infarction: altered excitation-contraction coupling. *Circulation* **104**, 688–693 https://doi.org/10.1161/hc3201.092285
15 Louch, W.E., Bito, V., Heinzel, F.R., Macianskiene, R., Vanhaecke, J., Flameng, W. et al. (2004) Reduced synchrony of Ca^{2+} release with loss of T-tubules-a comparison to Ca^{2+} release in human failing cardiomyocytes. *Cardiovasc. Res.* **62**, 63–73 https://doi.org/10.1016/j.cardiores.2003.12.031
16 Chaudhary, K.W., Rossman, E.I., Piacentino, V., Kenessey, I.I.I., Weber, A., Gaughan, C. et al. (2004) Altered myocardial Ca^{2+} cycling after left ventricular assist device support in the failing human heart. *J. Am. Coll. Cardiol.* **44**, 837–845 https://doi.org/10.1016/j.jacc.2004.05.049
17 Fukumoto, G.H., Lamp, S.T., Motter, C., Bridge, J.H., Garfinkel, A. and Goldhaber, J.I. (2005) Metabolic inhibition alters subcellular calcium release patterns in rat ventricular myocytes: implications for defective excitation-contraction coupling during cardiac ischemia and failure. *Circ. Res.* **96**, 551–557 https://doi.org/10.1161/01.RES.0000159388.61313.47
18 Song, L.S., Sobie, E.A., McCulle, S., Lederer, W.J., Balke, C.W. and Cheng, H. (2006) Orphaned ryanodine receptors in the failing heart. *Proc. Natl Acad. Sci. U.S.A.* **103**, 4305–4310 https://doi.org/10.1073/pnas.0509324103
19 Takeshima, H., Komazaki, S., Nishi, M., Iino, M. and Kangawa, K. (2000) Junctophilins: a novel family of junctional membrane complex proteins. *Mol. Cell* **6**, 11–22 https://doi.org/10.1016/s1097-2765(00)00003-4
20 Takeshima, H., Hoshijima, M. and Song, L.S. (2015) Ca^{2+} microdomains organized by junctophilins. *Cell Calcium* **58**, 349–356 https://doi.org/10.1016/j.ceca.2015.01.007
21 Gross, P., Johnson, J., Romero, C.M., Eaton, D.M., Poulet, C., Sanchez-Alonso, J. et al. (2021) Interaction of the joining region in junctophilin-2 with the L-type Ca^{2+} channel is pivotal for cardiac dyad assembly and intracellular Ca^{2+} dynamics. *Circ. Res.* **128**, 92–114 https://doi.org/10.1161/CIRCRESAHA.119.315715
22 Wei, S., Guo, A., Chen, B., Kutschke, W., Xie, Y.P., Zimmerman, K. et al. (2010) T-tubule remodeling during transition from hypertrophy to heart failure. *Circ. Res.* **107**, 520–531 https://doi.org/10.1161/CIRCRESAHA.109.212324
23 Guo, A., Zhang, X., Iyer, V.R., Chen, B., Zhang, C., Kutschke, W.J. et al. (2014) Overexpression of junctophilin-2 does not enhance baseline function but attenuates heart failure development after cardiac stress. *Proc. Natl Acad. Sci. U.S.A.* **111**, 12240–12245 https://doi.org/10.1073/pnas.1412729111
24 Zhang, C., Chen, B., Guo, A., Zhu, Y., Miller, J.D., Gao, S. et al. (2014) Microtubule-mediated defects in junctophilin-2 trafficking contribute to myocyte transverse-tubule remodeling and Ca^{2+} handling dysfunction in heart failure. *Circulation* **129**, 1742–1750 https://doi.org/10.1161/CIRCULATIONAHA.113.008452
25 Guo, Y., VanDusen, N.J., Zhang, L., Gu, W., Sethi, I., Guatimosim, S. et al. (2017) Analysis of cardiac myocyte maturation using CASAAV, a platform for rapid dissection of cardiac myocyte gene function *in vivo*. *Circ. Res.* **120**, 1874–1888 https://doi.org/10.1161/CIRCRESAHA.116.310283
26 Poulet, C., Sanchez-Alonso, J., Swiatlowska, P., Mouy, F., Lucarelli, C., Alvarez-Laviada, A. et al. (2021) Junctophilin-2 tethers T-tubules and recruits functional L-type calcium channels to lipid rafts in adult cardiomyocytes. *Cardiovasc. Res.* **117**, 149–161 https://doi.org/10.1093/cvr/cvaa033
27 Minamisawa, S., Oshikawa, J., Takeshima, H., Hoshijima, M., Wang, Y., Chien, K.R. et al. (2004) Junctophilin type 2 is associated with caveolin-3 and is down-regulated in the hypertrophic and dilated cardiomyopathies. *Biochem. Biophys. Res. Commun.* **325**, 852–856 https://doi.org/10.1016/j.bbrc.2004.10.107
28 Lyon, A.R., Nikolaev, V.O., Miragoli, M., Sikkel, M.B., Paur, H., Benard, L. et al. (2012) Plasticity of surface structures and beta(2)-adrenergic receptor localization in failing ventricular cardiomyocytes during recovery from heart failure. *Circ. Heart Fail.* **5**, 357–365 https://doi.org/10.1161/CIRCHEARTFAILURE.111.964692
29 Xu, M., Wu, H.D., Li, R.C., Zhang, H.B., Wang, M., Tao, J. et al. (2012) Mir-24 regulates junctophilin-2 expression in cardiomyocytes. *Circ. Res.* **111**, 837–841 https://doi.org/10.1161/CIRCRESAHA.112.277418
30 Chen, B., Li, Y., Jiang, S., Xie, Y.P., Guo, A., Kutschke, W. et al. (2012) beta-Adrenergic receptor antagonists ameliorate myocyte T-tubule remodeling following myocardial infarction. *FASEB J.* **26**, 2531–2537 https://doi.org/10.1096/fj.11-199505
31 Xie, Y.P., Chen, B., Sanders, P., Guo, A., Li, Y., Zimmerman, K. et al. (2012) Sildenafil prevents and reverses transverse-tubule remodeling and Ca2+ handling dysfunction in right ventricle failure induced by pulmonary artery hypertension. *Hypertension* **59**, 355–362 https://doi.org/10.1161/HYPERTENSIONAHA.111.180968
32 Wagner, E., Lauterbach, M.A., Kohl, T., Westphal, V., Williams, G.S., Steinbrecher, J.H. et al. (2012) Stimulated emission depletion live-cell super-resolution imaging shows proliferative remodeling of T-tubule membrane structures after myocardial infarction. *Circ. Res.* **111**, 402–414 https://doi.org/10.1161/CIRCRESAHA.112.274530
33 Zhang, H.B., Li, R.C., Xu, M., Xu, S.M., Lai, Y.S., Wu, H.D. et al. (2013) Ultrastructural uncoupling between T-tubules and sarcoplasmic reticulum in human heart failure. *Cardiovasc. Res.* **98**, 269–276 https://doi.org/10.1093/cvr/cvt030
34 Frisk, M., Ruud, M., Espe, E.K., Aronsen, J.M., Roe, A.T., Zhang, L. et al. (2016) Elevated ventricular wall stress disrupts cardiomyocyte t-tubule structure and calcium homeostasis. *Cardiovasc. Res.* **112**, 443–451 https://doi.org/10.1093/cvr/cvw111
35 Schobesberger, S., Wright, P., Tokar, S., Bhargava, A., Mansfield, C., Glukhov, A.V. et al. (2017) T-tubule remodelling disturbs localized beta2-adrenergic signalling in rat ventricular myocytes during the progression of heart failure. *Cardiovasc. Res.* **113**, 770–782 https://doi.org/10.1093/cvr/cvx074
36 Pinali, C., Malik, N., Davenport, J.B., Allan, L.J., Murfitt, L., Iqbal, M.M. et al. (2017) Post-myocardial infarction T-tubules form enlarged branched structures with dysregulation of junctophilin-2 and bridging integrator 1 (BIN-1). *J Am. Heart Assoc.* **6**, e004834 https://doi.org/10.1161/JAHA.116.004834
37 Wang, Y., Chen, B., Huang, C.K., Guo, A., Wu, J., Zhang, X. et al. (2018) Targeting calpain for heart failure therapy: implications from multiple murine models. *JACC Basic Transl. Sci.* **3**, 503–517 https://doi.org/10.1016/j.jacbts.2018.05.004
38 van Oort, R.J., Garbino, A., Wang, W., Dixit, S.S., Landstrom, A.P., Gaur, N. et al. (2011) Disrupted junctional membrane complexes and hyperactive ryanodine receptors after acute junctophilin knockdown in mice. *Circulation* **123**, 979–988 https://doi.org/10.1161/CIRCULATIONAHA.110.006437

39 Chen, B., Guo, A., Zhang, C., Chen, R., Zhu, Y., Hong, J. et al. (2013) Critical roles of junctophilin-2 in T-tubule and excitation-contraction coupling maturation during postnatal development. *Cardiovasc. Res.* **100**, 54–62 https://doi.org/10.1093/cvr/cvt180
40 Pedrozo, Z., Sanchez, G., Torrealba, N., Valenzuela, R., Fernandez, C., Hidalgo, C. et al. (2010) Calpains and proteasomes mediate degradation of ryanodine receptors in a model of cardiac ischemic reperfusion. *Biochim. Biophys. Acta* **1802**, 356–362 https://doi.org/10.1016/j.bbadis.2009.12.005
41 Letavernier, E., Zafrani, L., Perez, J., Letavernier, B., Haymann, J.P. and Baud, L. (2012) The role of calpains in myocardial remodelling and heart failure. *Cardiovasc. Res.* **96**, 38–45 https://doi.org/10.1093/cvr/cvs099
42 Murphy, R.M., Dutka, T.L., Horvath, D., Bell, J.R., Delbridge, L.M. and Lamb, G.D. (2013) Ca2+-dependent proteolysis of junctophilin-1 and junctophilin-2 in skeletal and cardiac muscle. *J. Physiol.* **591**, 719–729 https://doi.org/10.1113/jphysiol.2012.243279
43 Wu, C.Y., Chen, B., Jiang, Y.P., Jia, Z., Martin, D.W., Liu, S. et al. (2014) Calpain-dependent cleavage of junctophilin-2 and T-tubule remodeling in a mouse model of reversible heart failure. *J Am. Heart Assoc.* **3**, e000527 https://doi.org/10.1161/JAHA.113.000527
44 Guo, A., Hall, D., Zhang, C., Peng, T., Miller, J.D., Kutschke, W. et al. (2015) Molecular determinants of calpain-dependent cleavage of junctophilin-2 protein in cardiomyocytes. *J. Biol. Chem.* **290**, 17946–17955 https://doi.org/10.1074/jbc.M115.652396
45 Jiang, M., Hu, J., White, F.K.H., Williamson, J., Klymchenko, A.S., Murthy, A. et al. (2019) S-Palmitoylation of junctophilin-2 is critical for its role in tethering the sarcoplasmic reticulum to the plasma membrane. *J. Biol. Chem.* **294**, 13487–13501 https://doi.org/10.1074/jbc.RA118.006772
46 Guo, A., Wang, Y., Chen, B., Wang, Y., Yuan, J., Zhang, L. et al. (2018) E-C coupling structural protein junctophilin-2 encodes a stress-adaptive transcription regulator. *Science* **362**, eaan3303 https://doi.org/10.1126/science.aan3303
47 Lahiri, S.K., Quick, A.P., Samson-Couterie, B., Hulsurkar, M., Elzenaar, I., van Oort, R.J. et al. (2020) Nuclear localization of a novel calpain-2 mediated junctophilin-2 C-terminal cleavage peptide promotes cardiomyocyte remodeling. *Basic Res. Cardiol.* **115**, 49 https://doi.org/10.1007/s00395-020-0807-1
48 Croall, D.E. and DeMartino, G.N. (1991) Calcium-activated neutral protease (calpain) system: structure, function, and regulation. *Physiol. Rev.* **71**, 813–847 https://doi.org/10.1152/physrev.1991.71.3.813
49 Ono, Y. and Sorimachi, H. (2012) Calpains: an elaborate proteolytic system. *Biochim. Biophys. Acta* **1824**, 224–236 https://doi.org/10.1016/j.bbapap.2011.08.005
50 Ono, Y., Saido, T.C. and Sorimachi, H. (2016) Calpain research for drug discovery: challenges and potential. *Nat. Rev. Drug Discov.* **15**, 854–876 https://doi.org/10.1038/nrd.2016.212
51 Portbury, A.L., Willis, M.S. and Patterson, C. (2011) Tearin' up my heart: proteolysis in the cardiac sarcomere. *J. Biol. Chem.* **286**, 9929–9934 https://doi.org/10.1074/jbc.R110.170571
52 Sorimachi, H. and Ono, Y. (2012) Regulation and physiological roles of the calpain system in muscular disorders. *Cardiovasc. Res.* **96**, 11–22 https://doi.org/10.1093/cvr/cvs157
53 Luo, M. and Anderson, M.E. (2013) Mechanisms of altered Ca^{2+} handling in heart failure. *Circ. Res.* **113**, 690–708 https://doi.org/10.1161/CIRCRESAHA.113.301651
54 Guo, A., Fang, W. and Gibson, S. (2021) Sequence determinants of human junctophilin-2 protein nuclear localization and phase separation. *Biochem. Biophys. Res. Commun.* **563**, 79–84 https://doi.org/10.1016/j.bbrc.2021.05.078